MINERALOGICAL JOURNAL, VOL. 15, NO. 1, PP. 8–18, JANUARY 1990

Neutron diffraction study of babingtonite at 80K

Tokuhei TAGAI*, Werner JOSWIG and Hartmut FUESS**, [1]**

**Mineralogical Institute, Faculty of Science, University of Tokyo, 7-3-1 Hongo, Bunkyo-ku, Tokyo 113, Japan*

***Institut für Kristallographie der Universität Frankfurt am Main, Frankfurt am Main, Senckenberg-anlage 30, F.R.G.*

Abstract

The crystal structure of babingtonite was determined from neutron diffraction data at 80K. The lattice constants are $a = 7.497(1)$, $b = 12.225(1)$, $c = 6.710(1)$ Å, $\alpha = 86.18(1)$, $\beta = 93.90(1)$ and $\gamma = 112.27(1)°$ (at room temperature). The structure was refined assuming the space group symmetry of $P\bar{1}$. The cation distributions of Mn and Mg in Fe(1) site and Al in Fe(2) site were confirmed by applying the differences of the scattering lengths of the atoms in neutron diffraction. The accurate positions of the hydrogen atoms were determined.

Introduction

Babingtonite is a chain silicate and belongs to the pyroxenoid group. The pyroxenoid minerals can structurally be classified into two series according to the arrangements of the band of the cation octahedra (Takeuchi, 1976). One series is named as 'w-p' series consisting of wollastonite, rhodonite, pyroxmangite, pyroxferroite and ferrosilite III. The other series is the 'p-p' series of pectolite, serandite, babingtonite, Li-H-rhodonite and nambulite. The chemical formula for the w-p pyroxenoid series can generally be written as $M_N^{2+}Si_NO_{3N}$ and that for the p-p series can generally be expressed as $M_{N-1}M^{1+}HSi_NO_{3N}$. The p-p series is characterized not only by the arrangements of the cation octahedra but also by the presence of the hydrogen atoms.

The crystal structure of babingtonite was determined by Araki and Zoltai (1972). According to them, babingtonite has triclinic symmetry of space group $P\bar{1}$ and the structure contains two single chains of five SiO_4 tetrahedra, running parallel to [110], in the unit cell. The tetrahedral chains connect the polyhedral bands of Fe, Mn and Ca which are also connected between each other by the Ca polyhedra of an irregular form. Kosoi (1976) reinvestigated the structure. He found appreciable deviations from centrosymmetry in Fourier syntheses and determined the structure in space group P1.

The hydrogen atoms in the pyroxenoid minerals were found in the difference Fourier

[1]Present address: Fachbereich Materialwissenschaft, TH-Darmstadt, Petersenstr. 20, D-6100 Darmstadt, FRG

map by Takeuchi and Kudoh (1977) on pectolite from X-ray diffraction data. They proposed a statistical distribution of hydrogen atoms in two positions according to the elongated feature of the difference Fourier peaks in hydrogen positions. Ohashi and Finger (1981) determined the structure of santaclaraite, which is structurally related to rhodonite, babingtonite and nambulite. They could also locate hydrogen atoms in the difference Fourier map.

The cation distribution in babingtonite was studied by Amthauer (1980) using Mössbauer specta of ^{57}Fe between 30K and 600K. He concluded that Fe^{2+} occupies the Fe(1) site and Fe^{3+} occupies Fe(2) site. Mg and Mn, which are divalent, enter the Fe^{2+} sites and Al enters the Fe^{3+} site.

The aim of the present study is to determine the cation distribution of Fe and Mn atoms and a more accurate hydrogen position by means of neutron diffraction at 80K.

Experimental and results

Babingtonite from Yakuki Mine, Japan, was used for the present study. The sample was supplied from the collection of the University Museum, University of Tokyo (No. MI23055)

The chemical composition was determined by the electron probe micro-analysis (JEOL JCXA733, The Ocean Research Institute, University of Tokyo). The results of the analysis are listed in Table 1.

Neutron diffraction is not adequate to determine accurate lattice constants and therefore, they were determined from 24 reflections measured on a four circle diffractometer with MoKα radiation at room temperature as follows.

TABLE 1. Chemical composition of babingtonite

	wt%	atomic number for 150
SiO_2	53.32	4.93
TiO_2	-	-
Al_2O_3	0.65	0.08
FeO	21.82	1.75
MnO	2.20	0.18
MgO	0.27	0.05
CaO	19.59	2.00
Na_2O	0.07	0.03
K_2O	0.02	0.00
Cr_2O_3	0.07	0.00
V_2O_3	-	-
P_2O_5	0.24	0.03
total	98.25	

$a = 7.497(1)$, $b = 12.225(1)$, $c = 6.710(1)$ Å, $\alpha = 86.18(1)$, $\beta = 93.90(1)$ and $\gamma = 112.27(1)°$.

The reduced cell, which is different from this setting, has conventionally been used to the pyroxenoids and the present unit cell can be introduced with the transformation of $\vec{a}_k = -\vec{a}_r$, $\vec{b}_k = \vec{a}_r + \vec{b}_r$ and $\vec{c}_k = -\vec{c}_r$, where k and r mean the present cell and the reduced cell, respectively. The present unit cell setting is more convenient to discuss the pyroxenoid structure systematically because the pyroxenoid shows often two cleavages along the chains which run parallel to the b-axis with this section (Takeuchi, 1976).

Using a babingtonite single crystal of about 1.0 × 1.2 × 0.75 mm in size, the neutron diffraction data was collected on the four circle diffractometer D8 at High Flux Reactor of ILL, Grenoble, France. The wave length was 1.2668 Å from a Cu(220) monochromator. The intensity measurement was carried out at 80K in a C-1003 Displex cryostat. A total of 1642 independent reflections was collected up to $2\theta = 100°$ and supplied to the structure refinements.

The space group $P\bar{1}$ was assumed for the following structure refinement because the $P\bar{1}$ and P1 models are topologically identical and the deviation from centrosymmetry is only small. The number of parameters including anisotropic temperature factors is about 450 in the case of the P1 symmetry and it is not adequate, therefore, to refine the P1 structure with the limited number of reflections.

The structure was refined by the program XRAY-SYSTEM (Stewart *et al.*, 1972), with the parameters of Araki and Zoltai (1972) as starting values. The final R factor is 2.7% for 1642 reflections (including unobserved reflections). The final atomic

TABLE 2. Atomic coordinates

	x	y	z
Ca(1)	.1604(2)	.9423(2)	.8577(3)
Ca(2)	.2824(2)	.5201(1)	.6956(3)
Fe(1)	.0502(2)	.6440(1)	.9392(2)
Fe(2)	.1887(1)	.2353(1)	.8158(2)
Si(1)	.7651(3)	.0532(2)	.6590(4)
Si(2)	.8528(3)	.3133(2)	.5754(3)
Si(3)	.6389(3)	.4551(2)	.7904(3)
Si(4)	.7260(3)	.7134(2)	.6902(4)
Si(5)	.5085(3)	.8356(2)	.8940(4)
H	.2123(4)	.0956(2)	.5229(5)
O(1)	.7891(2)	.9874(1)	.4664(2)
O(2)	.9507(2)	.0803(1)	.8155(3)
O(3)	.7375(2)	.1711(1)	.5638(3)
O(4)	.0216(2)	.3382(1)	.7535(3)
O(5)	.0703(2)	.6203(1)	.6339(3)
O(6)	.6931(2)	.3707(1)	.6273(3)
O(7)	.4152(2)	.3844(1)	.8419(3)
O(8)	.7968(2)	.4753(1)	.9736(2)
O(9)	.6430(2)	.5686(1)	.6621(3)
O(10)	.8828(2)	.7553(1)	.8751(3)
O(11)	.1996(2)	.2208(1)	.5219(3)
O(12)	.5327(2)	.7369(1)	.7492(3)
O(13)	.2886(2)	.7989(1)	.9435(3)
O(14)	.3365(2)	.1424(1)	.9183(3)
O(15)	.5736(2)	.9675(1)	.7741(3)

coordinates and anisotropic temperature factors are given in Table 2 and Table 3, respectively. The selected interatomic distances and angles are listed in Table 4. The refined structure is shown in Fig. 1, drawn by the program of ORTEP (Johnson, 1976). Fig. 2-1 shows the schematic drawing of the tetrahedral chains and the octahedral bands

TABLE 3. Anisotropic temperature coefficients

	U11	U22	U33	U12	U13	U23
Ca(1)	.00126(8)	.00057(8)	.0008(1)	.00031(7)	.00012(9)	-.00015(9)
Ca(2)	.00059(8)	.00080(8)	.0008(1)	.00030(6)	.00019(9)	.00014(9)
Fe(1)	.00112(5)	.00114(5)	.00124(8)	.00042(4)	.00010(6)	-.00007(6)
Fe(2)	.00059(4)	.00054(4)	.00048(6)	.00022(3)	.00007(4)	.00003(4)
Si(1)	.00075(9)	.00044(9)	.0005(1)	.00026(7)	-.0001(1)	.0001(1)
Si(2)	.00066(9)	.00039(9)	.0003(1)	.00024(7)	-.0001(1)	-.0001(1)
Si(3)	.00059(9)	.00044(9)	.0003(1)	.00018(7)	.0000(1)	-.0000(1)
Si(4)	.00067(9)	.00037(9)	.0004(1)	.00021(7)	.0001(1)	.0001(1)
Si(5)	.00035(8)	.00042(9)	.0006(1)	.00009(7)	.0001(1)	-.0001(1)
H	.0038(2)	.0015(1)	.0019(2)	.0013(1)	.0005(2)	.0001(1)
O(1)	.00191(8)	.00077(8)	.0005(1)	.00061(6)	.00003(8)	-.00021(8)
O(2)	.00056(6)	.00078(6)	.00039(9)	.00019(5)	-.00015(7)	-.00001(7)
O(3)	.00109(7)	.00046(7)	.0009(1)	.00035(5)	-.00028(8)	-.00000(7)
O(4)	.00061(6)	.00074(6)	.00047(9)	.00027(5)	-.00017(8)	-.00014(7)
O(5)	.00091(7)	.00086(6)	.00050(9)	.00050(5)	.00033(8)	.00027(7)
O(6)	.00066(6)	.00068(6)	.00061(9)	.00044(5)	.00005(7)	-.00007(7)
O(7)	.00054(6)	.00054(6)	.00067(9)	.00023(5)	.00026(7)	.00023(7)
O(8)	.00069(6)	.00075(7)	.0006(1)	.00046(5)	-.00008(7)	-.00015(7)
O(9)	.00064(7)	.00037(6)	.0009(1)	.00013(5)	-.00023(8)	-.00015(7)
O(10)	.00056(7)	.00068(6)	.00044(9)	.00021(5)	.00001(7)	-.00011(7)
O(11)	.00128(7)	.00067(7)	.00040(9)	.00036(6)	.00037(8)	.00018(8)
O(12)	.00072(7)	.00068(7)	.00051(9)	.00037(5)	.00008(7)	-.00018(7)
O(13)	.00061(7)	.00068(7)	.0011(1)	.00021(5)	.00028(8)	-.00010(8)
O(14)	.00095(7)	.00065(6)	.00053(9)	.00039(5)	-.00037(8)	-.00024(7)
O(15)	.00087(7)	.00051(7)	.00098(9)	.00030(6)	.00020(8)	.00029(8)

TABLE 4. Selected bond distances and angles

Ca(1)-O(1)	2.291(3)	Fe(2)-O(2)	2.057(1)	Si(4)-O(9)	1.661(2)		
O(2)	2.364(3)	O(4)	2.096(2)	O(10)	1.619(3)		
O(2)*	2.703(3)	O(7)	1.978(1)	O(11)	1.615(3)		
O(10)	2.448(2)	O(10)	2.201(2)	O(12)	1.660(3)		
O(13)	2.326(3)	O(11)	2.004(2)				
O(14)	2.351(2)	O(14)	1.936(2)	Si(5)-O(12)	1.669(3)		
O(15)	3.058(3)			O(13)	1.592(3)		
O(15)*	3.087(3)	Si(1)-O(1)	1.623(3)	O(14)	1.620(3)		
		O(2)	1.630(3)	O(15)	1.668(2)		
Ca(2)-O(4)	2.375(2)	O(3)	1.620(3)				
O(5)	2.353(3)	O(15)	1.634(2)	H -O(1)	1.010(4)		
O(6)	2.453(3)			O(11)	1.571(4)		
O(7)	2.375(3)	Si(2)-O(3)	1.630(2)				
O(8)	2.349(3)	O(4)	1.637(3)				
O(9)	2.566(2)	O(5)	1.605(3)				
O(9)*	2.873(2)	O(6)	1.667(3)				
O(12)	2.640(2)						
		Si(3)-O(6)	1.633(3)				
Fe(1)-O(4)	2.214(2)	O(7)	1.611(2)				
O(5)	2.114(2)	O(8)	1.609(3)				
O(8)	2.205(2)	O(9)	1.682(3)				
O(8)*	2.229(2)						
O(10)	2.184(2)						
O(13)	2.058(2)						

---

* Atoms in equivalent positions

TABLE 4. Selected bond distances and angles (continued)

O(1)-Ca(1)-O(2)	158.60(13)	
O(1)	O(2)*	78.23(13)
O(1)	O(10)	110.77(10)
O(1)	O(13)	112.66(12)
O(1)	O(14)	81.44(8)
O(1)	O(15)	127.61(8)
O(1)	O(15)*	73.49(8)
O(2)	O(2)*	80.47(11)
O(2)	O(10)	73.17(7)
O(2)	O(13)	88.73(9)
O(2)	O(14)	88.00(9)
O(2)	O(15)	56.65(9)
O(2)	O(15)*	122.54(9)
O(2)*	O(10)	95.41(7)
O(2)*	O(13)	167.16(9)
O(2)*	O(14)	65.59(9)
O(2)*	O(15)	104.31(9)
O(2)*	O(15)*	136.70(9)
O(10)	O(13)	74.67(7)
O(10)	O(14)	155.58(13)
O(10)	O(15)	120.80(10)
O(10)	O(15)*	124.95(10)
O(13)	O(14)	121.30(10)
O(13)	O(15)	74.92(6)
O(13)	O(15)*	55.57(6)
O(14)	O(15)	55.21(10)
O(8)-Ca(2)-O(12)	85.31(8)	
O(9)	O(9)*	67.92(9)
O(9)	O(12)	60.04(6)
O(9)*	O(12)	110.34(6)
O(4)-Fe(1)-O(5)	170.60(8)	
O(4)	O(8)	95.28(7)
O(4)	O(8)*	80.81(7)
O(4)	O(10)	80.41(8)
O(4)	O(13)	93.10(8)
O(5)	O(8)	90.70(9)
O(5)	O(8)*	93.01(9)
O(5)	O(10)	93.26(8)
O(5)	O(13)	93.39(8)
O(8)	O(8)*	80.99(9)
O(8)	O(10)	174.96(7)
O(8)	O(13)	96.78(10)
O(8)*	O(10)	95.68(7)
O(8)*	O(13)	173.25(10)
O(10)	O(13)	86.10(7)
O(2)-Fe(2)-O(4)	92.61(7)	
O(2)	O(7)	174.91(10)
O(2)	O(10)	84.64(7)
O(2)	O(11)	88.06(7)
O(2)	O(14)	87.12(7)
O(4)	O(7)	87.56(7)
O(4)	O(10)	82.66(8)
O(9)-Si(4)-O(10)	113.00(15)	
O(9)	O(11)	108.27(16)
O(9)	O(12)	103.35(11)
O(10)	O(11)	114.43(12)
O(10)	O(12)	107.05(16)
O(11)	O(12)	110.15(16)
O(12)-Si(5)-O(13)	110.15(12)	
O(12)	O(14)	109.07(16)
O(12)	O(15)	110.26(16)
O(13)	O(14)	109.07(17)
O(13)	O(15)	106.46(15)
O(14)	O(15)	103.51(12))
O(1)- H -O(11)	174.5(3)	

O(14)-Ca(1)-O(15)*	78.19(7)	
O(15)	O(15)*	70.28(9)
O(4)-Ca(2)-O(5)	91.33(8)	
O(4)	O(6)	120.78(9)
O(4)	O(7)	72.87(7)
O(4)	O(8)	75.11(8)
O(4)	O(9)	131.61(10)
O(4)	O(9)*	89.64(10)
O(4)	O(12)	160.02(12)
O(5)	O(6)	64.02(8)
O(5)	O(7)	159.85(10)
O(5)	O(8)	81.64(9)
O(5)	O(9)	136.38(8)
O(5)	O(9)*	112.14(8)
O(5)	O(12)	81.77(8)
O(6)	O(7)	134.84(11)
O(6)	O(8)	141.16(11)
O(6)	O(9)	83.91(8)
O(6)	O(9)*	58.20(8)
O(6)	O(12)	72.88(7)
O(7)	O(8)	82.22(9)
O(7)	O(9)	61.91(7)
O(7)	O(9)*	80.89(7)
O(8)	O(9)	112.77(9)
O(8)	O(9)*	159.97(9)
O(4)-Fe(2)-O(11)	89.27(8)	
O(4)	O(14)	170.71(10)
O(7)	O(10)	90.34(7)
O(7)	O(11)	97.02(7)
O(7)	O(14)	91.89(7)
O(10)	O(11)	168.85(8)
O(10)	O(14)	88.07(8)
O(11)	O(14)	100.00(9)
O(1)-Si(1)-O(2)	111.03(16)	
O(1)	O(3)	103.94(16)
O(1)	O(15)	109.01(13)
O(2)	O(3)	113.59(12)
O(2)	O(15)	108.20(15)
O(3)	O(15)	110.89(16)
O(3)-Si(2)-O(4)	108.53(15)	
O(3)	O(5)	114.47(16)
O(3)	O(6)	107.15(12)
O(4)	O(5)	113.52(12)
O(4)	O(6)	110.53(16)
O(5)	O(6)	102.30(15)
O(6)-Si(3)-O(7)	111.20(13)	
O(6)	O(8)	109.97(16)
O(6)	O(9)	104.19(15)
O(7)	O(8)	117.88(16)
O(7)	O(9)	101.24(15)
O(8)	O(9)	111.23(12)

f the babingtonite structure. A tetrahedral chain links two octahedral bands, which re tied by a Ca-polyhedron to one another, constructing a layer-like structure and it lso links the octahedral bands to those of the neighboring layers.

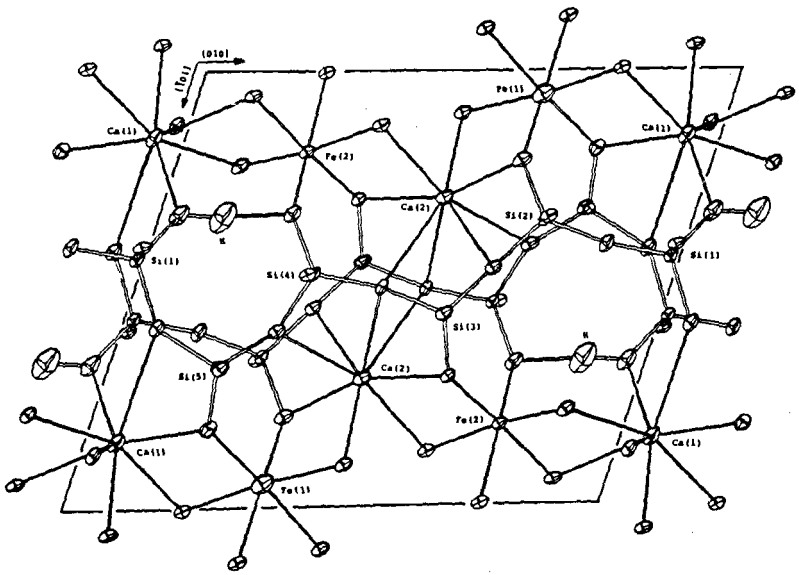

FIG. 1. Crystal structure of babingtonite projected on [010]-[101].

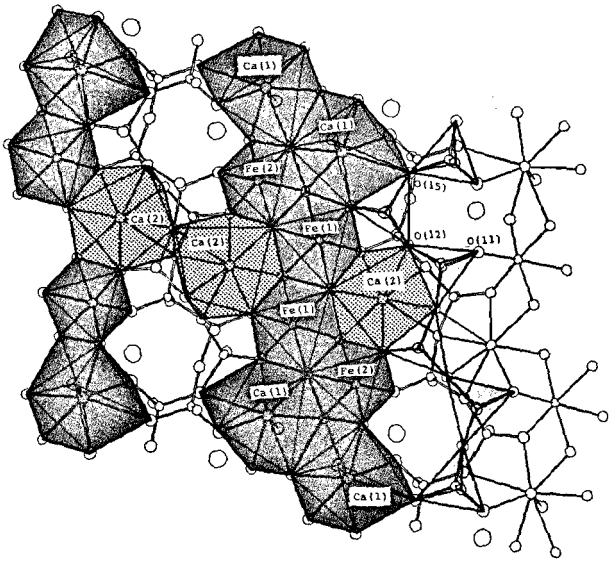

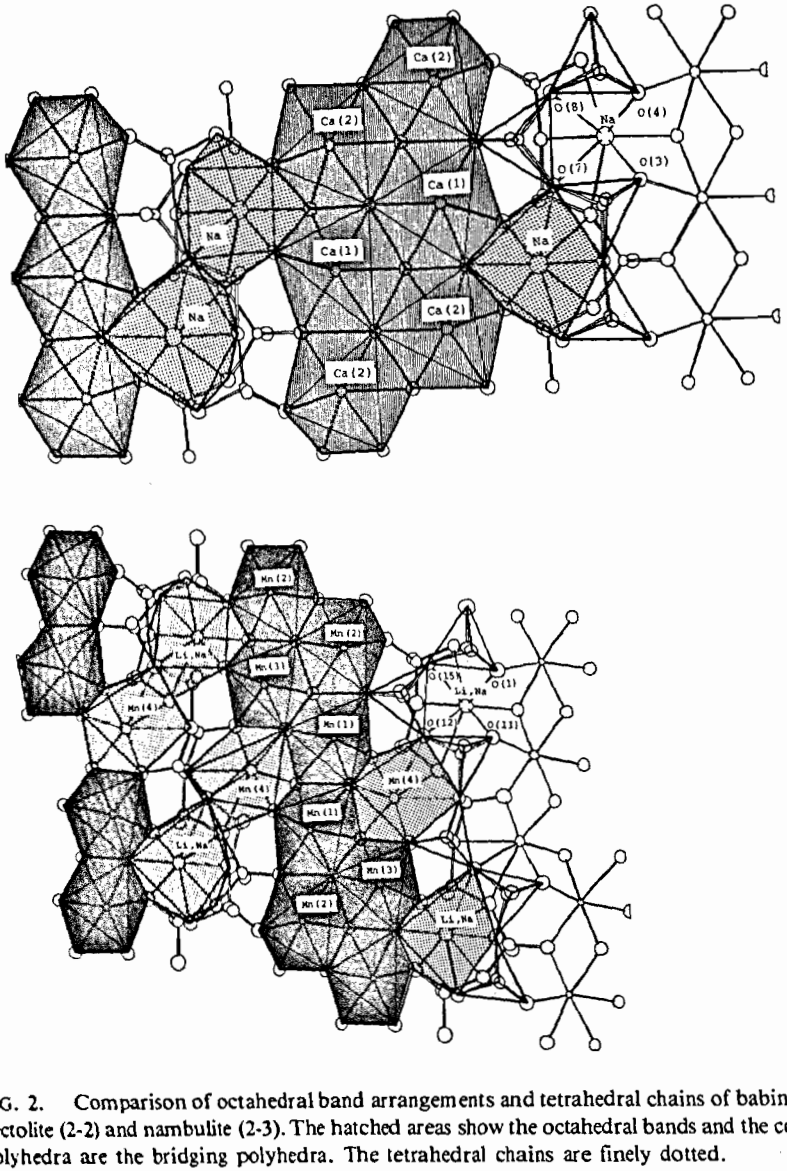

FIG. 2. Comparison of octahedral band arrangements and tetrahedral chains of babingtonite (2-1), pectolite (2-2) and nambulite (2-3). The hatched areas show the octahedral bands and the coarsely dotted polyhedra are the bridging polyhedra. The tetrahedral chains are finely dotted.

Cation ordering

According to the chemical analysis and specific gravity (Nambu *et al.*, 1969), Araki and Zoltai (1972) postulated substitutions of (Ca, Mn, Na, K), (Fe^{2+}, Mn, Mg), (Fe^{3+}, Al) and (Si, Al). Amthauer (1980) assumed the substitution of Fe^{2+} by Mn^{2+} and Mg^{2+} and that of Fe^{3+} by Al^{3+} from the results of the Mössbauer spectra. In our study, the

TABLE 5. Final population parameters

	population parameters (refined)	(calculated)	
Ca(1)	0.99 (1)	0.99	$Ca_{1.00}{}^{+Na}{}_{.02}$
Ca(2)	1.01 (1)	1.00	$Ca_{1.00}{}^{+Na}{}_{.01}$
Fe(1)	0.79 (1)	0.78	$Fe_{.82}{}^{+Mn}{}_{.18}{}^{+Mg}{}_{.05}$
Fe(2)	0.98 (1)	0.98	$Fe_{.93}{}^{+Al}{}_{.08}$
Si(1)	1.004(1)	0.99	$Si_{.99}$
Si(2)	0.998(1)	0.99	$Si_{.99}$
Si(3)	1.004(1)	0.99	$Si_{.99}$
Si(4)	1.002(1)	0.99	$Si_{.99}$
Si(5)	1.004(1)	0.99	$Si_{.99}$

cation distributions were directly refined from the difference of the scattering length of the atoms in neutron diffraction. Neutron diffraction is sometimes very useful to determine the site occupations of the neighboring atoms in the periodic table. Fe and Mn show almost the same scattering factors in X-ray diffraction but their scattering lengths in neutron diffraction are 0.96 and −0.36 (10^{-12}cm), respectively. The location of hydrogen atom and its occupation probability can also be determined by neutron diffraction, for example in staurolite (Tagai and Joswig, 1985). The site occupancies were determined by refining the population parameters which are linearly dependent to the scattering lengths of the atoms. The final population parameters of cations and the calculated values based on the cation distribution are listed in Table 5.

Fe(1) and Fe(2) polyhedra show the population parameters of 0.79(1) and 0.98(1), respectively. This low occupation parameter of 0.79 can only be attained by the substitution Fe/Mn because of the negative scattering length of Mn. Together with the results of Mössbauer spectra (Amthauer, 1980), it can be concluded that the divalent Fe occupies the Fe(1)-site, which is substituted by divalent Mn and Mg and that the trivalent Fe occupies Fe(2)-site, which may be substituted by Al. If occupations of all Al atoms in Fe(2) site and all Mn and Mg atoms in Fe(1) site are assumed, the most probable distributions of Fe atoms satisfying the observed population parameters can be attained by; ($Fe_{0.82}Mn_{0.18}Mg_{0.05}$) for Fe(1) and ($Fe_{0.93}Al_{0.08}$) for Fe(2). These occupations yield the population parameters 0.78 and 0.98 for Fe(1) and Fe(2), respectively. Ca-octahedra, Ca(1) and Ca(2), show the population parameters of 0.99(1) and 1.01(1), respectively. If Ca is substituted by all the Na and K atoms, the population parameters changes only about 1/100, because the sample contains very small amounts of Na and K. Therefore, it can be assumed that Na and K atoms occupy Ca(1) and Ca(2) sites. Si(1), Si(2), Si(3), Si(4) and Si(5) show the population parameters of 1.004(1), 0.998(1), 1.004(1), 1.002(1) and 1.004(1), respectively. It indicates that all the Si tetrahedra show full occupation

of Si and practically no substitution of Al.

From these considerations, the most probable chemical formula was obtained as follows:

$[Ca_{2.00}, Na_{0.01}][Fe_{0.82}, Mn_{0.18}, Mg_{0.05}]^{2+}[Fe_{0.93}, Al_{0.08}]^{3+}\ Si_{4.93}O_{14}(OH)$.

In this chemical formula, the valence neutrality is not strictly maintained. It may be explained by the experimental errors in the chemical analysis and the errors in the least squares refinements.

Hydrogen atom

The existence of hydrogen atoms in pyroxenoid of p-p sries is essential but the accurate position of the hydrogen atom has not been determined. The hydrogen was located on the difference Fourier map in pectolite (Takeuchi and Kudoh, 1977) and santaclaraite (Ohashi and Finger, 1981) using X-ray diffraction data. In this study the location of hydrogen atom was directly determined applying its relatively large negative scattering length on neutron diffraction (-0.378×10^{-12} cm). On the Fourier map the location of the hydrogen atom was clearly found between O(1) and O(11) and the accurate position of the hydrogen atom was refined by least squares methods. According to the results of the least squares refinements, the bond distances of O(1)-H, O(11)-H and O(1)-O(11) are 1.010, 1.571 and 2.579 Å, respectively. The angle of O(1)-H-O(11) is 174.50°. This geometry is classified as a medium to strong hydrogen bonding. On the difference Fourier map, Takeuchi and Kudoh (1977) found two peaks in the hydrogen position which they interpreted as statistical distribution of the hydrogen atom into two positions. In our study, however, no such separated peaks on the difference Fourier map nor large anisotropic temperature coefficients of hydrogen atom were observed, as similar to the observation by Ohashi and Finger (1981) in santaclaraite.

Discussion

The structural principle of babingtonite is similar with those of other pyroxenoid minerals of p-p series. A tetrahedral chain links two octahedral bands, which are also tied by the cation polyhedra to each other, constructing layer-like structure (Fig. 2). In Fig. 2, the hatched areas are the octahedral bands and the coarsely dotted polyhedra are the bridging polyhedra. In babingtonite the bridging cation polyhedra are Ca ones and in the other p-p pyroxenoids the bridging polyhedra are Na-Na polyhedra in pectolite, Li-Mn one in nambulite and Li-Li one in Li-H-rhodonite. These monovalent cation polyhedra share their edges with those of the C-shaped tetrahedral chains, O(3)-O(7)-O(8)-O(4) in pectolite and O(11)-O(12)-O(15)-O(1) in nambulite (Fig. 2-2,3). In babingtonite, however, the C-shaped tetrahedral chain does not share its edges, O(11)-O(12)-O(15)-O(1) in Fig. 2-1, with any bridging cation polyhedron. It may be explained as

follows. Babingtonite lacks monovalent cation and the monovalent cation site remains vacant, which may be the characteristic structural feature of babingtonite in p-p series of pyroxenoid. The lack of monovalent cation is balanced by the existence of the trivalent Fe.

The bond distance between O(1) and O(11) is 2.578 Å and the bond angle of O(1)-H-O(11) is 174.5°. The corresponding O-O distances in the other pyroxenoid minerals are 2.473 Å for pectolite (Takeuchi and Kudoh, 1977), 2.453 Å for serandite (Takeuchi *et al.*, 1976), 2.464 Å for nambulite (Narita *et al.*, 1975) and 2.449 Å for Li-H-rhodonite (Murakami *et al.*, 1975). These short bond lengths in the C-shape Si-O-Si chain and the existence of strong hydrogen bonds between those oxygens are the characteristic structural feature of the p-p pyroxenoid. The longer bond distance of O(1)-O(11) in babingtonite is due to the fact that the O(1)-O(11) is the polyhedron edge of the vacant site as mentioned above.

Acknowledgments—One of the authors (T.T.) thanks Alexander von Humboldt-Foundation (Bonn) for Financial support to carry out a part of this work during his stay in Federal Republic Germany. The sample was kindly supplied by the University Museum, University of Tokyo. The computations were carried out at Rechenzentrum der Universität Frankfurt am Main and the Computer Center of University of Tokyo.

This work was supported in part by funds from the Cooperative Program (No. 88145) provided by Ocean Research Institute, University of Tokyo.

References

AMTHAUER, G. (1980): ^{57}Fe Mössbauer study of babingtonite. *Am. Mineral.*, **65**, 157-162.

ARAKI, T. and ZOLTAI, T. (1972): Crystal structure of babingtonite. *Z. Krist.*, **135**, 355-373.

JOHNSON, C.K. (1976): *ORTEP II: FORTRAN thermal ellipsoid plot program for crystal structure illustrations.* Rep. ORNL-5138, Oak Ridge National Lab., Tennessee.

KOSOI, A.L. (1976): The structure of babingtonite. *Sov. Phys. Crystallogr.*, **20**, 446-451.

MURAKAMI, T., TAKEUCHI, Y., TAGAI, T. and KOTO, K. (1977): Lithium-hydrorhodonite. *Acta Cryst.*, **B33**, 919-921.

NAMBU, M., TANIDA, K. and KITAMURA, T. (1969): Mineralogical study of manganese silicate ores in Northern Japan. VII. Manganiferous babingtonite from Yakuki mine, Fukushima Prefecture. *Senko-Seiren Kenkyusho Iho.*, **25**, 117-128.

NARITA, H., KOTO, K. and MORIMOTO, N. (1975): The crystal structure of nambulite $(Li,Na)Mn_4Si_5O_{14}(OH)$. *Acta Cryst.*, **B31**, 2422-2426.

OHASHI, Y. and FINGER, L.W. (1981): The crystal structure of santaclaraite, $CaMn_4[Si_5O_{14}(OH)](OH)\cdot H_2O$: the role of hydrogen atoms in the pyroxenoid structure. *Am. Mineral.*, **66**, 154-168.

STEWART, D.B., KRUGER, G.J., AMMON, H.L., DICKINSON, C. and HALL, S.R. (1972): *The XRAY system.* Computer Sci. Center Univ. Maryland.

TAGAI, T. and JOSWIG, W. (1985): Untersuchung der Kationenverteilung im Staurolith durch Neutronenbeugung bei 100K. *N. Jb. Miner. Mh.*, **H3**, 97-107.

TAKEUCHI, Y. (1976): Two structure series of pyroxenoids. *Proc. Japan Academy*, **52**, 122-125.